

# Demonstration of Real-time Cognitive Radar using Spectrally-Notched Random FM Waveforms

Jonathan W. Owen<sup>1</sup>, Charles A. Mohr<sup>1,2</sup>, Benjamin H. Kirk<sup>3,4</sup>, Shannon D. Blunt<sup>1</sup>,  
Anthony F. Martone<sup>4</sup>, Kelly D. Sherbondy<sup>4</sup>

<sup>1</sup>Radar Systems Lab (RSL), University of Kansas, Lawrence, KS

<sup>2</sup>Sensors Directorate, Air Force Research Laboratory (AFRL), Wright-Patterson AFB, OH

<sup>3</sup>Electrical Engineering Dept., Pennsylvania State University, University Park, PA

<sup>4</sup>Army Research Laboratory (ARL), Adelphi, MD

**Abstract**—With the reality of increasing radio frequency (RF) spectral congestion, radar systems capable of dynamic spectrum sharing are needed. Recent work has demonstrated a real-time cognitive capability on a software defined radio (SDR) by generating pulse-agile LFM chirps that vary their center frequency and bandwidth to avoid dynamic interference on a per-pulse basis. Separately, spectral notching of random FM waveforms was developed and experimentally evaluated as another means with which to mitigate emulated interference, though real-time operation had not yet been demonstrated.

Here the operational framework of the former is combined with the waveform agility of the latter to facilitate real-time generation of notched, random FM waveforms as part of an integrated cognitive SDR architecture. This implementation supports pulse repetition frequencies up to 2.2 kHz for on-the-fly waveform synthesis, can incorporate multiple spectral notches per waveform, and can achieve notch depths of 25 dB relative to peak power (with greater depth possible given greater computational resources). Performance examples are illustrated along with implementation decisions and design trade-offs.

**Keywords**—*spectrum sharing, cognitive radar, spectrum notching, waveform diversity, real-time operation*

## I. INTRODUCTION

Cognitive radar, also known as fully adaptive radar, is generally understood to refer to systems that in some sense learn and subsequently respond to attributes of their operational environment [1, 2]. Due to increasing spectral congestion and competition [3], an important topic of research is the use of cognition in a spectrum sharing context [4] to modify the radar’s physical emission structure according to sensed RF interference (RFI) in the band of interest (e.g. [5–8]). Essentially, these efforts are working to develop “good spectral neighbor” capabilities for the radar by mitigating the mutual interference to/from other spectrum users.

A separate, yet related, research direction has focused on the radar utilization of emerging software-defined radio (SDR) platforms (e.g. [9, 10]) due to their cost-effectiveness, scalability, and the prospect of rapid prototyping. Specifically, a growing body of work is devoted to the application of SDRs to realize real-time cognitive radar capabilities (e.g. [8, 11–13]). For example, it was recently shown that by utilizing a rapid band-aggregation method [6] to monitor RFI and select appropriate usable subbands, subsequent linearly frequency modulated (LFM) chirp waveforms could be generated via

direct digital synthesis (DDS) on an Ettus x310 SDR to avoid interferers in real-time [8].

The purpose of this paper is to demonstrate how another cognitive radar capability for spectrum sharing can likewise be deployed for real-time mutual interference mitigation. Where the approach in [8] involves a sense-and-avoid (SAA) strategy, this other approach [7] employs a sense-and-notch (SAN) strategy that leverages recent work on spectrally-shaped, random FM waveforms (see [14] and references therein) to place in-band spectral notches on a per-waveform basis in response to dynamic RFI. Based on emulated (i.e. not real-time) RFI it was previously experimentally shown using test equipment that spectral notches having better than 50 dB in depth (relative to the peak spectrum power) can be achieved for these physically realizable waveforms [7, 15].

It was noted in [11] that a key enabler to realizing spectral notching that is responsive on a per-pulse timescale is implementation of waveform generation on the field-programmable gate array (FPGA) of the SDR. When in-band RFI is dynamically changing during the radar’s coherent processing interval (CPI), these SAA or SAN capabilities must likewise perform at the rate of the pulse repetition frequency (PRF). Consequently, here the SAN method [6, 7], which also leverages aspects of the SAA deployment from [8], is implemented on the FPGA of an Ettus x310 SDR and demonstrated for real-time operation.

## II. COGNITIVE SPECTRAL NOTCHING VIA THE SDR

In [7] it was experimentally demonstrated, albeit not yet at real-time, that random FM waveforms possessing deep spectral notches could be physically realized according to the available in-band spectrum determined using the fast spectrum sensing (FSS) method of [6]. This particular class of waveforms [14] is attractive in this context because they provide tremendous design freedom and flexibility (due to non-repetition) while their FM structure ensures compatibility with high-power transmitters.

Of course, nothing comes for free. It has been observed that changing the radar emission structure during the CPI in response to dynamic RFI does introduce a significant clutter modulation effect [7]. That said, a variety of recent receive processing methods have been developed and experimentally demonstrated to compensate for this effect with varying efficacy [16–19], with additional efforts ongoing.

Implementation of the SAN capability on an SDR platform is accomplished by sequentially applying two random FM waveform generation methods. First, the pseudo-random optimized (PRO) FM approach of [20] is employed to produce a transmitter-suitable waveform that possesses a desirable overall power spectrum shape (Gaussian is useful for this purpose) and containing spectral notches [7] based on the RFI determination from FSS [6]. However, because PRO-FM generally cannot achieve very significant notch depths by itself (20 dB at best), further notch suppression is required.

In [7] it was shown that the reiterative uniform weighted optimization (RUWO) method [21] could accomplish this task, though the attendant computation cost is rather high. Then in [15] the analytical spectrum notching (ASpeN) approach was developed and experimentally demonstrated using a high-fidelity arbitrary waveform generator (AWG) to achieve notch depths better than 50 dB.

Most recently, ASpeN has been modified for use on the more modest digital-to-analog conversion (DAC) rates, and thus lower fidelity, available in SDRs. The resulting zero-order reconstruction optimization of waveforms (ZOROW) method [22] accounts for much, though not all, of the distortion arising from this lower fidelity, which is particularly important when attempting to form spectral notches.

The notched waveform generation approach implemented on the SDR's FPGA is therefore summarized as follows. Let  $T$  be the pulse width,  $B$  the 3-dB bandwidth, and  $f_s$  the SDR's DAC rate. For radar applications it is presumed that  $B$  is a significant fraction of the DAC rate, and thus interpolation has limited benefit (see [22]). Denote  $\bar{\mathbf{s}}_q$  as the length- $N$  digital representation of the desired analog waveform  $s_q(t)$  that the SDR is intended to produce for the  $q$ th of  $Q$  pulses in the CPI. Moreover, denote  $\bar{\mathbf{s}}_q^{(k)}$  as the version of this vector after  $k$  iterations of the PRO-FM alternating projections [20]

$$\bar{\mathbf{r}}_q^{(k+1)} = \mathbb{F}^{-1} \left\{ \bar{\mathbf{g}} \odot \exp \left( j \angle \mathbb{F} \left\{ \bar{\mathbf{s}}_q^{(k)} \right\} \right) \right\} \quad (1)$$

and

$$\bar{\mathbf{s}}_q^{(k+1)} = \bar{\mathbf{u}} \odot \exp \left( j \angle \bar{\mathbf{r}}_q^{(k+1)} \right), \quad (2)$$

where  $\bar{\mathbf{s}}_q^{(0)}$  is a random initialization (constant amplitude and uniformly distributed in phase). Here  $\mathbb{F}$  and  $\mathbb{F}^{-1}$  are the Fourier and inverse Fourier transforms, respectively,  $\angle(\bullet)$  extracts the phase of the argument, and  $\odot$  is the Hadamard product. The length- $N$  vector  $\bar{\mathbf{g}}$  is a discretization of the desired spectral template  $|G(f)|$ , while the length- $N$  vector  $\bar{\mathbf{u}}$  is a discretization of rectangular window  $u(t)$  that has duration  $T$ .

The desired power spectrum  $|G(f)|^2$ , which is arbitrary in general, is chosen to be Gaussian so that the associated waveform autocorrelation is also approximately Gaussian. The spectral intervals of in-band RFI determined by FSS [6], represented as  $\Omega$ , are used to place notches in this template via

$$|G(f)| = 0 \text{ for } f \in \Omega. \quad (3)$$

Imposing the null constraint in (3) via the alternating projections of (1) and (2) can produce spectral notches with depths up to 20 dB. Moreover, this process can require hundreds of iterations that would generally preclude real-time operation. Therefore, in this implementation notched PRO-FM via (1)-(3) is used to roughly shape the entire waveform spectrum, including the formation of shallow notches, and then ZOROW [22] is applied to complete the notching process. It has been found that at least initiating notch formation with PRO-FM facilitates faster convergence for subsequent ZOROW application, which is likewise iterative.

The ZOROW formulation operates on the version of the discretized waveform at the  $k = K$  terminal iteration, which we shall denote as

$$\mathbf{s}_q = \exp(j\boldsymbol{\phi}_q), \quad (4)$$

where

$$\boldsymbol{\phi}_q = [\phi_{q,1} \ \phi_{q,2} \ \cdots \ \phi_{q,N}]^T. \quad (5)$$

This signal representation conforms to the zero-order hold model employed by the SDR DAC, in which the DAC input sample is held constant for  $T_s$  seconds. The resulting analog signal is then fed through a reconstruction filter to suppress the repeated images outside the fundamental frequency interval of  $[-f_s/2, +f_s/2]$ .

It was shown in [15] that perfect Nyquist reconstruction can be realized for a pulsed (i.e. time-limited) signal given sufficient sampling of the analytical spectrum. For the ZOROW waveform representation [22], this sampled analytical spectrum has the form

$$S_q(f_m, \boldsymbol{\phi}_q) = \frac{\sin(\pi f_m T_s)}{\pi f_m} \sum_{n=1}^N \exp \left( -j(2\pi f_m (n-1/2)T_s + \phi_{q,n}) \right), \quad (6)$$

where  $f_m = m\Delta f$  for integer  $m$  on the interval  $-\infty < m < \infty$ , as long as  $\Delta f \leq 1/(2T)$ . Noting that (6) takes the form of a discrete Fourier transform (DFT) with an imposed sinc( $\cdot$ ) envelope, it can be calculated efficiently using a fast Fourier transform (FFT).

The ZOROW formulation [22] then employs the cost function

$$J = \sum_m |S_q(f_m; \boldsymbol{\phi}_q)|^2, \quad (7)$$

where the summation corresponds to the frequency interval(s) from (3) for which notching is required. The gradient of (7) with respect to  $\boldsymbol{\phi}_q$  is then determined [22] for use in gradient-descent optimization as

$$\boldsymbol{\phi}_q^{(\ell+1)} = \boldsymbol{\phi}_q^{(\ell)} + \mu_\ell \mathbf{p}_q^{(\ell)}, \quad (8)$$

where  $\mu_\ell$  is the step-size based on a simple backtracking technique [23], and

$$\mathbf{p}_q^{(\ell)} = \begin{cases} -\mathbf{g}_0 & \text{when } k = 0 \\ -\mathbf{g}_q^{(\ell)} + \beta \mathbf{p}_q^{(\ell-1)} & \text{otherwise} \end{cases} \quad (9)$$

is the search direction at the  $l$ th iteration. Here  $0 < \beta < 1$  dictates the type of gradient-descent being used and it can be shown that (9) can be efficiently computed via

$$\mathbf{g}_q^{(\ell)} = 2\Im\left\{\tilde{\mathbf{A}}^H(\tilde{\mathbf{s}}_{f,q}^{(\ell)} \odot \tilde{\mathbf{w}}) \odot \mathbf{s}_q^{*(\ell)}\right\}. \quad (10)$$

Here  $\Im(\cdot)$  extracts the imaginary part of the argument,  $\tilde{\mathbf{A}}^H$  is the  $(2N-1) \times N$  truncated inverse DFT matrix,  $(\cdot)^*$  denotes complex conjugation,  $\mathbf{s}_q^{(\ell)}$  is the discrete vector from (4) at the  $l$ th iteration of ZOROW, with  $\tilde{\mathbf{s}}_{f,q}^{(\ell)}$  the corresponding Fourier transform after padding with  $N-1$  zeros, and  $\tilde{\mathbf{w}}$  is the length  $2N-1$  vector representing the sinc( $\cdot$ ) envelope in (6) with the unnotched portions replaced by zeros. With the gradient expressed in this manner it can be efficiently computed using FFTs [24, 25].

The gradient-descent implementation in [15, 22] relies on a “heavy ball” framework [26] with a backtracking technique [23] to select the step-size. However, backtracking involves determination of cost function values that can be inefficient to compute on an FPGA. That said, it has been observed for this formulation that the use of standard steepest descent ( $\beta = 0$ ) combined with backtracking via a simple line-search method tends to converge quickly to a constant step-size value. Thus  $\mu_\ell$  is set to 1 for this FPGA implementation, which has been found to be less than the smallest optimized step-size obtained by backtracking.

As an example, Fig. 1 illustrates the root mean-squared (RMS) power spectra of  $Q = 1000$  random FM waveforms containing a central spectral notch location spanning 10% of the band. These waveforms were generated using only  $K = 2$  PRO-FM iterations and either  $L = 6$  or 1000 ZOROW iterations. Significant notch depth can clearly be achieved via  $L = 1000$ , though we shall use the  $L = 6$  case for FPGA implementation.

Figure 2 compares this particular implementation in terms of convergence over 1000 iterations to other gradient-descent approaches [27] when a spectral notch is placed in the center of

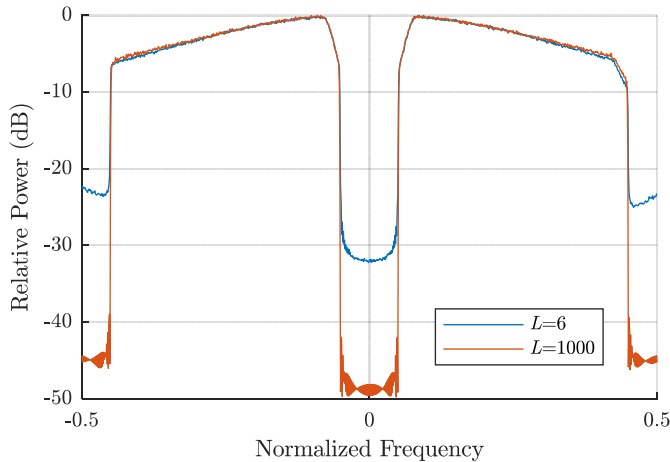


Fig. 1. RMS power spectra of PRO-FM / ZOROW waveform sets for a central notch location spanning 10% of the band after  $K = 2$  PRO-FM iterations and  $L = 6$  and 1000 ZOROW iterations. Per [22], notches are also placed at the band edges to facilitate spectral containment prior to DAC reconstruction.

the spectrum. While the heavy ball scheme (yellow trace) is the best overall after 1000 iterations, this simple approach involving straightforward steepest descent (SD) without backtracking yields the best performance after the first 100 iterations. Since real-time operation limits the number of feasible iterations, this streamlined approach is clearly an attractive solution.

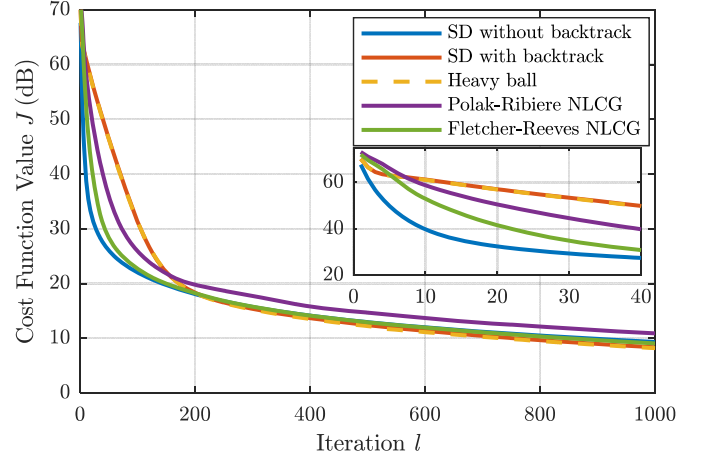


Fig. 2. Comparison of cost-function (7) minimization for various gradient-descent methods

### III. IMPLEMENTATION CONSIDERATIONS

A block diagram of the SDR cognitive radar architecture is shown in Fig. 3. The RF environment is sensed at the receive port of the SDR, where the signal is frequency down-converted and quantized into in-phase & quadrature channels at 100 MSamples/s, processed by a high throughput FFT performed on the FPGA, and then continuously streamed to the host computer. Currently FSS [6] is performed on the host computer to identify the spectral locations of RFI within the 100 MHz band during the radar listening periods. The identified RFI spectral locations are then returned to the SDR, where the PRO-FM / ZOROW notched waveform generation process is performed.

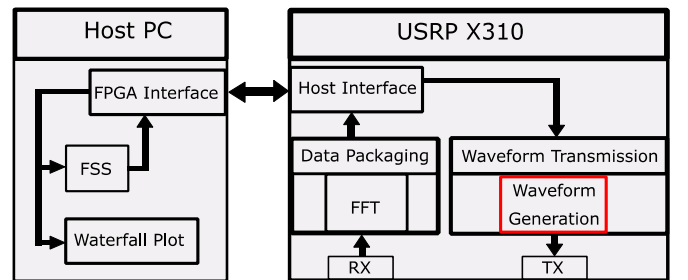


Fig. 3. Cognitive radar architecture on the SDR. See [8] for further details.

The maximum time  $T_{\text{PRI}}$  required to generate each waveform establishes the minimum feasible pulse repetition interval (PRI) and thus the maximum PRF for cognitive operation. However, a latency also exists between the observance of changes in the RFI and when FSS responds with the appropriate notch locations, which currently establishes the

minimum adaptation interval  $T_{\text{adapt}}$ . Consequently, while a new waveform is generated on a per-PRI basis, the notch locations for each waveform are currently updated by FSS at a rate of once every  $R$  PRIs (depending on the PRF employed). Figure 4 exemplifies a timing diagram of the SDR operation where the RFI changes every 4 PRIs and  $R = 3$  PRIs.

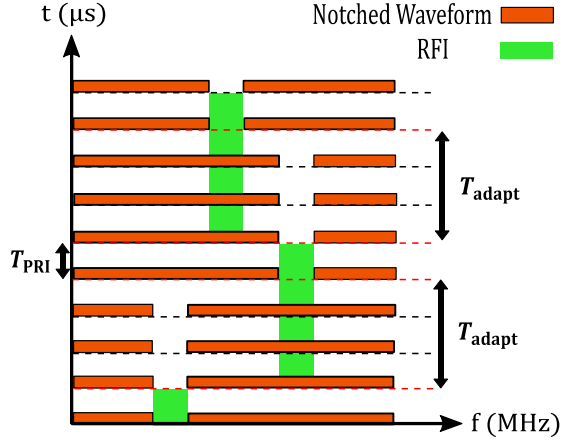


Fig. 4. Timing diagram of SAN cognitive radar adjusting a spectral notch location to coincide with dynamic RFI, where  $T_{\text{adapt}} = 3T_{\text{PRI}}$

The FPGA code architecture was developed such that board resources are conservatively utilized, timing constraints imposed by the PRI ( $< 1$  ms desired) are met, and notch depths in the waveform are maximized under these conditions. As such, 2 iterations of PRO-FM was deemed sufficient to impose a preliminary spectral shape followed by 6 iterations of ZOROW, thereby realizing  $\sim 25$  dB of notch depth relative to peak power. As illustrated in Fig. 1, greater notch depth could be achieved on the SDR, though doing so would alter the response time trade-space. With this parameterization, the SDR supports cognitive spectral notching at a PRF up to 2.2 kHz, a minimum adaptation interval of 3 ms, and can incorporate multiple spectral notches per waveform. Thus the adaptation rate  $R$  is presently 7 PRIs at the highest PRF supported.

All FPGA processing, including the implementations of PRO-FM and ZOROW for notched waveform generation, is performed using FFTs, inverse FFTs, multiplies, and additions in a burst streaming format compatible with a commercial off-the-shelf (COTS) SDR. The final FPGA resource utilization was at  $\sim 30\%$ , thereby providing the possibility for additional upgrades.

#### IV. EVALUATION OF REAL-TIME OPERATION

To characterize the behavior of the real-time cognitive SAN architecture on the SDR, various RFI patterns were generated and resulting performance assessed. The SDR operates at a center frequency of 2 GHz and measures complex baseband data after receive down-conversion based on a 100 MHz sample clock. The SAN implementation has an adaptation interval of  $R = 7$  PRIs, a pulse duration of  $2.56 \mu\text{s}$ , and PRI of  $450.6 \mu\text{s}$ .

The RFI test cases include 1) three swept-frequency tones with 15 ms or 5 ms dwell times, 2) three independent 5 MHz bands of OFDM subcarriers randomly hopping with dwell

times of 15 ms, and 3) one contiguous 40 MHz band of OFDM subcarriers randomly hopping with a dwell time of 15 ms. An independent arbitrary waveform generator (AWG) is used to generate the RFI scenarios that are combined with the radar transmissions in closed loop for subsequent cognitive radar performance testing.

Figure 5 shows a spectral capture of three independent frequency tones (Case 1) as well as a corresponding notched random FM waveform generated by the SDR. Figure 6 shows a waterfall spectrogram (frequency content versus PRI time) when the RFI dwell time is 15 ms. With a response time of 3 ms the SAN cognitive radar is able to respond relatively quickly and form multiple notches that coincide with the sensed RFI.

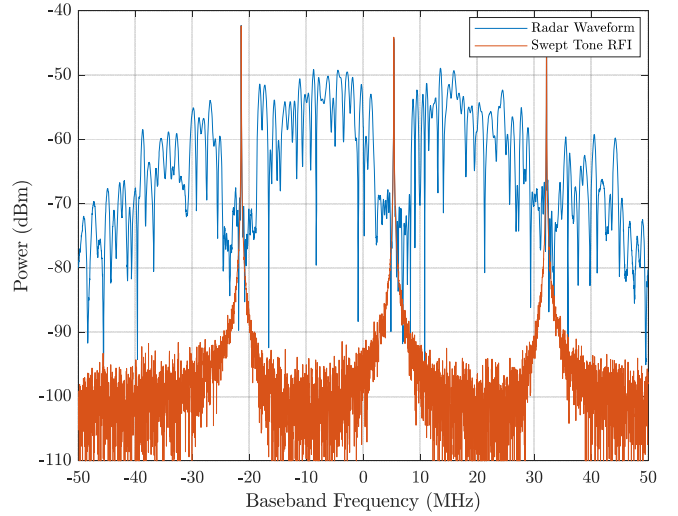


Fig. 5. (Case 1) Spectrum capture showing three tonal interferers (red) and the SAN radar spectrum (blue) with collocated notches.

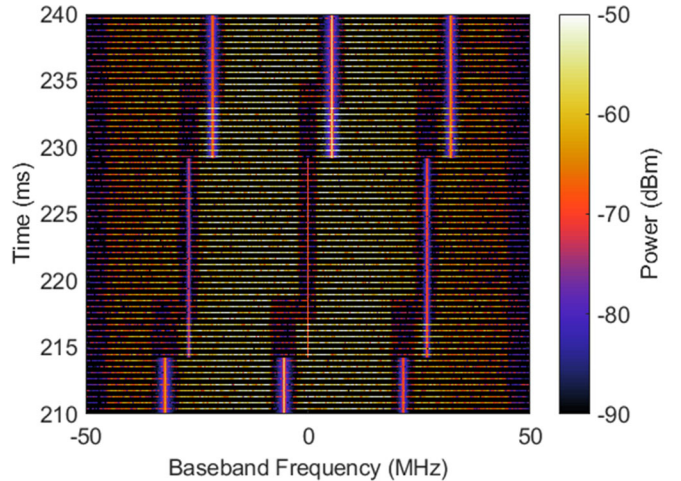


Fig. 6. (Case 1a) Waterfall spectrogram versus PRI time for RFI comprised of three stepped tones (vertical pink bars) and the SAN radar spectrum (horizontal yellow lines) with notches. The RFI changes every 15 ms.

For the same case, when the dwell time of the three swept tones is commensurate with the adaptation speed of this SAN implementation, notching alignment accuracy is observed to degrade rather significantly (Fig. 7). For this reason, ongoing work is investigating how adaptation latency can be further

reduced. For environments in which the RFI exhibits observable patterns, prediction is being explored as means to anticipate where notching is likely to be required so that corresponding waveform generation can be initiated earlier [28].

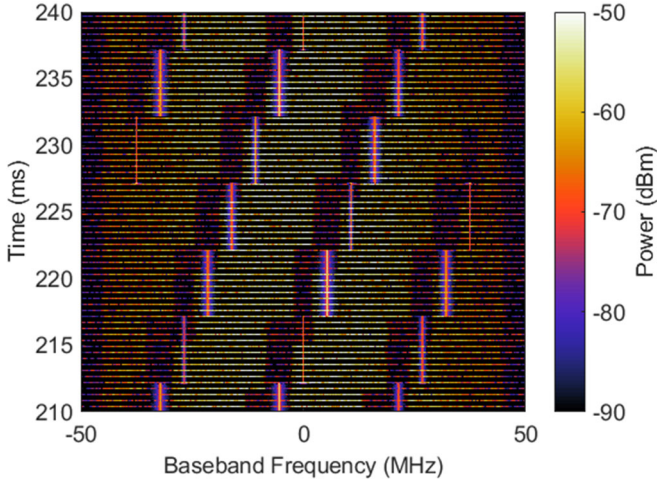


Fig. 7. (Case 1b) Waterfall spectrogram versus PRI time for RFI comprised of three stepped tones (vertical pink bars) and the SAN radar spectrum (horizontal yellow lines) with notches. The RFI changes every 5 ms.

Figure 8 shows a scenario in which the RFI consists of three 5 MHz bands comprised of OFDM subcarriers (Case 2) that change spectral locations randomly every 15 ms. The same 7-PRI latency is again observed, with the notch widths and locations adjusting according to the observed RFI. For randomly changing RFI, presuming no discernible pattern is available, this manner of reactive mode is more appropriate than a predictive mode (like [28]).

Moreover, while the persistent RFI around  $-33$  MHz is a random occurrence in these results, such an outcome could occur more frequently in practice if the RFI is likewise employing some form of dynamic spectrum access. Specifically, the two systems could potentially achieve a steady-state condition in which it is more beneficial from a mutual signal-to-interference-plus-noise (SINR) perspective for both the radar and the other user to maintain the same spectral disposition. Of course, this manner of “locked in” behavior may be contraindicated by the need for spectral maneuver freedom.

Finally, Fig. 9 shows the cognitive SAN radar adapting to a single 40 MHz band of OFDM subcarriers (Case 3) that changes spectral locations randomly every 15 ms. The 7-PRI adaptation latency is once again observed. However, this result highlights the fact that, while transmit spectral notching generally permits more overall bandwidth to be preserved and is more robust to clutter modulation relative to a sense-and-avoid (SAA) mode [29, 19], the SAA may still be preferred in some instances. Specifically, the time interval from 210 to 223 ms in Fig. 9 illustrates that SAN provides access to both sides of the remaining bandwidth. However, when significant RFI content is present in an off-center portion of the available band (223 to 240 ms and beyond in Fig. 9) the SAA approach would realize essentially the same spectral content as SAN at a lower

computational cost, which would translate into lower response latency. The determination of whether to use SAA or SAN, in a reactive or predictive mode, is part of a higher level “meta-cognition” study that is also ongoing [30].

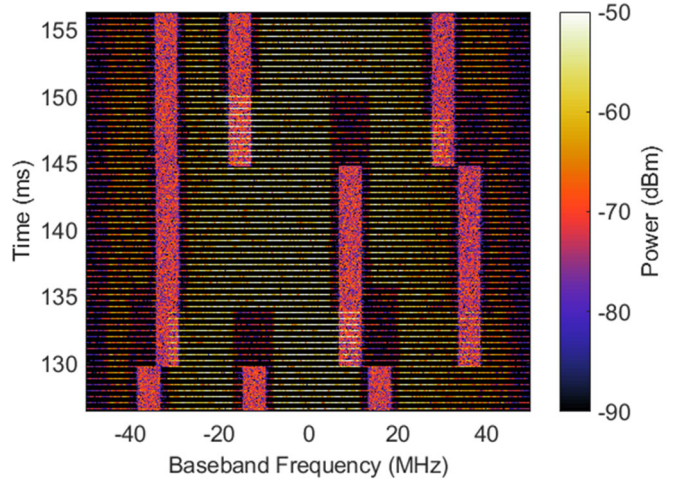


Fig. 8. (Case 2) Waterfall spectrogram versus PRI time for RFI comprised of three 5 MHz bands of OFDM subcarriers (vertical pink bars) and the SAN radar spectrum (horizontal yellow lines) with notches. The RFI changes every 15 ms.

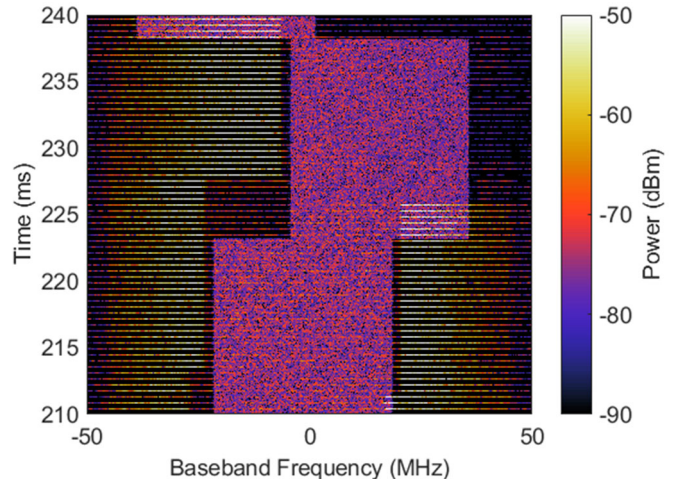


Fig. 9. (Case 3) Waterfall spectrogram versus PRI time for RFI comprised of one 40 MHz band of OFDM subcarriers (vertical pink bar) and the SAN radar spectrum (horizontal yellow lines) with notches. The RFI changes every 15 ms.

## V. CONCLUSIONS

A sense-and-notch (SAN) cognitive radar approach involving the use of spectrally notched, random FM waveforms has been implemented and demonstrated for real-time operation on a COTS SDR. The waveform generation process only requires simple FPGA resource blocks including FFTs, multiplications, and additions. The resulting SDR architecture supports PRFs up to 2.2 kHz, can incorporate multiple spectral notches per waveform, and achieves notch depths of 25 dB relative to peak power. The evaluation of this capability for operational radar modes such as moving target indication (MTI) in the presence of dynamic RFI is anticipated in the near future.

## REFERENCES

- [1] J.R. Guerci, *Cognitive Radar: The Knowledge-Aided Fully Adaptive Approach*, Artech House, Inc., 2010.
- [2] A. Farina, A. De Maio, S. Haykin, *The Impact of Cognition on Radar Technology*, SciTech Publishing, 2017.
- [3] H. Griffiths, L. Cohen, S. Watts, E. Mokole, C. Baker, M. Wicks, S. Blunt, "Radar spectrum engineering and management: technical and regulatory issues," *Proc. IEEE*, vol. 103, no. 1, pp. 85-102, Jan. 2015.
- [4] S.D. Blunt, E.S. Perrins, *Radar & Communication Spectrum Sharing*, SciTech Publishing, 2018.
- [5] P. Stinco, M.S. Greco, F. Gini, "Spectrum sensing and sharing for cognitive radars," *IET Radar, Sonar & Navigation*, vol. 10, no. 3, pp. 595-602, Feb. 2016.
- [6] A. Martone, K. Ranney, K. Sherbondy, K. Gallagher, S. Blunt, "Spectrum allocation for non-cooperative radar coexistence," *IEEE Trans. Aerospace & Electronic Systems*, vol. 54, no. 1, pp. 90-105, Feb. 2018.
- [7] B. Ravenscroft, J.W. Owen, J. Jakabosky, S.D. Blunt, A.F. Martone, K.D. Sherbondy, "Experimental demonstration and analysis of cognitive spectrum sensing and notching for radar," *IET Radar, Sonar & Navigation*, vol. 12, no. 12, pp. 1466-1475, Dec. 2018.
- [8] B.H. Kirk, R.M. Narayanan, K.A. Gallagher, A.F. Martone, K.D. Sherbondy, "Avoidance of time-varying radio frequency interference with software-defined cognitive radar," *IEEE Trans. Aerospace & Electronic Systems*, vol. 55, no. 3, pp. 1090-1107, June 2019.
- [9] B.L. Cheong, R. Palmer, Y. Zhang, M. Yeary, T.-Y. Yu, "A software-defined radar platform for waveform design," *IEEE Radar Conf.*, Atlanta, GA, May 2012.
- [10] K. El-Darymli, N. Hansen, B. Dawe, E.W. Gill, W. Huang, "Design and implementation of a high-frequency software-defined radar for coastal ocean applications," *IEEE Aerospace & Electronic Systems Mag.*, vol. 33, no. 3, pp. 14-21, Mar. 2018.
- [11] J.M. Christiansen, G.E. Smith, K.E. Olsen, "USRP based cognitive radar testbed," *IEEE Radar Conf.*, Seattle, WA, May 2017.
- [12] J.M. Christiansen, K.E. Olsen, G.E. Smith, "Fully adaptive radar for track update-interval control," *IEEE Radar Conf.*, Oklahoma City, OK, Apr. 2018.
- [13] J.M. Christiansen, G.E. Smith, "Parameter selection in a fully adaptive tracking radar," *Intl. Radar Conf.*, Toulon, France, Sept. 2019.
- [14] S.D. Blunt, J.K. Jakabosky, C.A. Mohr, P.M. McCormick, J.W. Owen, B. Ravenscroft, C. Sahin, G.D. Zook, C.C. Jones, J.G. Metcalf, T. Higgins, "Principles & applications of random FM radar waveform design," to appear in *IEEE Aerospace & Electronic Systems Magazine*.
- [15] C.A. Mohr, S.D. Blunt, "Analytical spectrum representation for physical waveform optimization requiring extreme fidelity," *IEEE Radar Conf.*, Boston, MA, Apr. 2019.
- [16] B. Ravenscroft, et al, "Optimal mismatched filtering to address clutter spread from intra-CPI variation of spectral notches," *IEEE Radar Conf.*, Boston, MA, Apr. 2019.
- [17] J. Owen, B. Ravenscroft, S.D. Blunt, "Devoid clutter capture and filling (DeCCaF) to compensate for intra-CPI spectral notch variation," *Intl. Radar Conf.*, Toulon, France, Sept. 2019.
- [18] B.H. Kirk, A.F. Martone, K.D. Sherbondy, R.M. Narayanan, "Mitigation of target distortion in pulse-agile sensors via Richardson-Lucy deconvolution," *Electronics Letters*, vol. 55, no. 23, pp. 1249-1252, Nov. 2019.
- [19] B. Ravenscroft, J.W. Owen, B.H. Kirk, S.D. Blunt, A.F. Martone, K.D. Sherbondy, R.M. Narayanan, "Experimental assessment of joint range-Doppler processing to address clutter modulation from dynamic radar spectrum sharing," *IEEE Intl. Radar Conf.*, Washington, DC, Apr. 2020.
- [20] J. Jakabosky, S.D. Blunt, B. Himed, "Spectral-shape optimized FM noise radar for pulse agility," *IEEE Radar Conf.*, Philadelphia, PA, May 2016.
- [21] T. Higgins, T. Webster, A.K. Shackelford, "Mitigating interference via spatial and spectral nulling," *IET Radar, Sonar & Navigation*, vol. 8, no. 2, pp. 84-93, Feb. 2014.
- [22] C. Mohr, J.W. Owen, S.D. Blunt, "Zero-order reconstruction optimization of waveforms (ZOROW) for modest DAC-rate systems," *IEEE Intl. Radar Conf.*, Washington, DC, Apr. 2020.
- [23] J. Nocedal, S. Wright. *Numerical Optimization*, Springer Science & Business Media, 2006.
- [24] B. O'Donnell, J.M. Baden, "Fast gradient descent for multi-objective waveform design," *IEEE Radar Conf.*, Philadelphia, PA, May 2016.
- [25] D. Zhao, Y. Wei, Y. Liu, "Spectrum optimization via FFT-based conjugate gradient method for unimodular sequence design," *Signal Processing*, vol. 142, pp. 354-365, Jan. 2018.
- [26] E. Ghadimi, R. Feyzmahdavian, M. Johansson, "Global convergence of the heavy-ball method for convex optimization," *European Control Conf.*, Linz, Austria, July 2015
- [27] W.W. Hager, H. Zhang, "A survey of nonlinear conjugate gradient methods," *Pacific Journal of Optimization*, vol. 2, no. 1, pp. 35-58, Dec. 2005.
- [28] J. Kovariksiy, J.W. Owen, R.M. Narayanan, S.D. Blunt, A.F. Martone, K.D. Sherbondy, "Spectral prediction and notching of RF emitters for cognitive radar coexistence," *IEEE Intl. Radar Conf.*, Washington, DC, Apr. 2020.
- [29] B.H. Kirk, M.A. Kozy, K.A. Gallagher, R.M. Narayanan, R.M. Buehrer, A.F. Martone, K.D. Sherbondy, "Cognitive software-defined radar: evaluation of target detection with RFI avoidance," *IEEE Radar Conf.*, Boston, MA, Apr. 2019.
- [30] A.F. Martone, et al, "Metacognition for radar coexistence," *IEEE Intl. Radar Conf.*, Washington, DC, Apr. 2020.